

UNCLASSIFIED

Defense Technical Information Center
Compilation Part Notice

ADP014042

TITLE: STAP for SAR

DISTRIBUTION: Approved for public release, distribution unlimited
Availability: Hard copy only.

This paper is part of the following report:

TITLE: Military Application of Space-Time Adaptive Processing [Les applications militaires du traitement adaptatif espace-temps]

To order the complete compilation report, use: ADA415645

The component part is provided here to allow users access to individually authored sections of proceedings, annals, symposia, etc. However, the component should be considered within the context of the overall compilation report and not as a stand-alone technical report.

The following component part numbers comprise the compilation report:

ADP014040 thru ADP014047

UNCLASSIFIED

STAP for SAR

A. Farina

Technical Directorate, Radar & Technology Division

Alenia Marconi Systems

Via Tiburtina Km. 12.400, 00131 Rome, Italy

tel: +39-06-4150-2279; fax: +39-06-4150-2665, e.mail: afarina@amsjv.it

Key words: moving target detection and imaging, Synthetic Aperture Radar, Space Time adaptive processing.

1. SUMMARY

This paper describes the application of STAP (Space Time Adaptive Processing) to Synthetic Aperture Radar (SAR) systems. SAR is a microwave sensor that allows us to have a high resolution mapping of electromagnetic (e.m.) backscatter from an observed scene. A two-dimensional image is provided in the radar polar coordinates, i.e.: slant range and azimuth. High resolution in slant range is obtained by transmitting a coded waveform, with a large value of the time - bandwidth product, and coherently processing the echoes in a filter matched to the waveform. High resolution along the transversal direction is achieved by forming a synthetic aperture. This requires: (i) to put the radar on board of a moving platform, e.g.: an aircraft or a satellite; (ii) to record the e.m. signals from each scatterer which is illuminated by the moving antenna beam in successive instants of time, and (iii) to coherently combine the signals - via a suitable azimuthal matched filter - thus focusing the sliding antenna pattern in a narrower synthetic beam [AUS84]. The advantage of combining SAR and STAP is evident: the detected moving target is shown on top on the SAR image of the sensed scene. The paper is organised as follows. The description of the technical problem to tackle is in section 2; also a look to the state of the art is included. It is well known that the SAR image of a moving target presents a number of aberrations: these are briefly reviewed in section 3. Signal processing schemes are described in Section 4 which is the core of the paper. We move from a suitable modification of the conventional MTI and Pulse Doppler (PD), to Along Track Interferometry (ATI) SAR, to Displaced Phase Center Antenna (DPCA) - the predecessor of STAP. Finally the last described processing scheme is the one that combines the data in the three domains: space, time and frequency. Some of the schemes are tested with simulated data. The paper concludes with a perspective to future work, and a collection of references for further readings.

2. DESCRIPTION OF THE PROBLEM AND STATE OF THE ART

In many applications (e.g.: surveillance) of SAR, it is desirable to detect and possibly produce focused images of moving objects. A moving low RCS object is not easily detectable against strong echoes scattered from an extended fixed scene. When detected, its resulting image is smeared and ill positioned with respect to the stationary background. These shortcomings are a direct consequence of the SAR image formation process. The cross-range high resolution in a SAR is obtained by taking advantage of the relative motion, supposed known, between the sensor and the scene. If, however, there is an object moving in an unpredictable manner, the image formation process does not function properly. Basically, the main degradations due to the target motion are the following. (i) The range migration through adjacent resolution cells (due to the radial velocity of target respect to radar) causes a reduction of the signal-to-clutter power ratio, which can seriously impair the detection capabilities. Furthermore, range migration causes a decrease in the integration time and a consequent loss of resolution. (ii) Even in the absence of range migration, or after its correction, the phase shift induced by the motion causes: an ill-positioning (along track) of the target image with respect to ground, mainly owing to

the range component of the relative radar-target velocity; a smearing of the image is also due to the uncompensated cross-range velocity and/or range acceleration.

A first possibility that has been studied of discriminating the moving target signals from the fixed scene returns is on the basis of their different Doppler frequency spectra; see, for instance, [DDB94] and the quoted references. In fact, the target spectrum has a Doppler centroid approximately linearly proportional to the along-range velocity of target and a spectrum width depending on the azimuthal velocity and the radial acceleration components of target. Assuming that the radar pulse repetition frequency (PRF) is high enough to make available a region in the Doppler frequency domain not occupied by the stationary scene, the method works as follows (see Section 4.1 for details). First transform a sequence of radar target returns to the frequency domain. Second, locate spectral bands, outside the narrow band frequency around origin corresponding to stationary scene, and determine the centre frequencies of such bands. Third, translate each outlying spectral band to the origin, convert the resulting signal back to the time domain and correlate with the reference function of the conventional SAR. The correlator output will show the peaks in the correct locations of the targets. A refinement of this basic technique aims at the image formation of each target: it is obtained by matching also the width, not only the mean value, of spectral band outside the stationary scene Doppler spectrum. The method suffers however of three shortcomings. (i) it requires the use of a high PRF which causes a corresponding reduction of the SAR swath width and an increase of the data throughput. (ii) It does not correctly focus the image of a target having a quite arbitrary path. The spectrum of the target echoes alone is not sufficient; we need to know the instantaneous phase law to form the synthetic aperture with respect to the moving target. (iii) It does not succeed with a target whose motion has a small range velocity component, so that its spectrum is superimposed on the clutter (i.e.: on the stationary scene) spectrum. A distinct advantage of this system is related to the possibility to use it with conventional, non multi-channel phased-array radar antennas.

More powerful methods have been conceived to overcome these drawbacks; they are based on the use of more than one antenna, on board the moving platform, to cancel the clutter and detect the slowly moving targets. The radar system uses an array of antennas, mounted on the platform along the flight direction, and corresponding receiving channels. This makes available a certain number of space samples (echoes received from different antenna elements) and time samples (echoes collected at different time instants). These echoes are coherently combined, with proper weights, in a space-time processor to cancel the echo backscattered from the ground and enhance the target echo. Space-time effectively reduces the lower bound on the minimum detectable target velocity that would be established by using only frequency filtering. It measures the relative phase between two or more coherent signals, received from different antennas, rather than the Doppler frequency shift within a single receiving channel. Instead of using a mono-dimensional filtering, clutter cancellation is the result of a powerful two-dimensional (in the temporal frequency, i.e.: Doppler, and in the spatial frequency, i.e.: azimuth angle) filtering. Furthermore this method does not require necessarily to work with high PRF values. This is the STAP approach: see [WAR94], [KLE98] and [KLE99] for details. The way to the full fledged STAP wasn't immediate: it passed to the ATI applied to SAR (described in Section 4.2) and to the DPCA (see Section 4.3); both techniques being essentially based on the use of the echoes captured by two antennas.

A refinement of ATI-SAR was the VSAR (Velocity SAR) method [FPO97]. In a way similar to the progression from a two-pulse canceller to a bank of Doppler filters to reject clutter and detect moving targets in a conventional search radar, the technique can be generalised to a linear array of identical antennas. For each channel a complex SAR image is calculated. A Fourier transform along the physical aperture (i.e.: the channel number) is applied to each pixel, and this corresponds to a multiple beam former. For each Fourier cell the related image shows the scene for a certain range of radial velocities (velocity SAR image [FPO97]). This method hasn't however originally designed to suppress clutter, since no attempt is made to subtract signals. The requirement to cancel the echoes from stationary scatterers leads directly to adaptive space-time filtering.

Once detected the presence of a moving target, we have to estimate its phase modulation law to be able to form a high resolution image of it. A method for providing the estimate is by means of time-frequency analysis

of the received signal. This, combined with STAP, brings to the joint space-time-frequency processing presented in detail in Section 4.4. The time-frequency representation is obtained by evaluating the Wigner-Ville Distribution (WVD) of the signal. This distribution is a signal representation consisting in the mapping of the signal onto a plane whose coordinates are time and frequency. The WVD, in particular, produces a mapping such that the signal energy is concentrated along the curve of the instantaneous frequency. This frequency is obtained as the centre of gravity of the WVD; the instantaneous phase is derived by integration of the instantaneous frequency. The clutter echoes are cancelled by the adaptive space-time processor, where the space-time covariance matrix of clutter is estimated on-line and used to evaluate the optimal weights of the two-dimensional filter. The time-frequency analysis provides an estimation of the instantaneous frequency of the possibly present moving target, and – by integration – the original instantaneous phase. The phase is used to compensate for the shift due to the relative target-radar motion.

3. ABERRATIONS DUE TO TARGET MOTION

There are some interesting effects that occur with moving targets. A moving target with a radial component of velocity v_r results in a Doppler shift on each echo of

$$f_D = \frac{2v_r f_0}{c} \quad (1)$$

where f_0 is the radar carrier frequency and c is the velocity of propagation. Thus the Doppler history of the sequence of echoes is shifted in frequency (Figure 1), and is matched filtered (with a small mismatch) with an azimuth shift which is the product of the Doppler shift and the slope of the Doppler history

$$f_D \frac{r\lambda}{2v/d} = \frac{v_r r}{v} \quad (2)$$

where v is the platform speed, r is the platform-target range and d is the along track dimension of the antenna (the real aperture). It is well known that an image from an aircraft-borne SAR of a moving train having a component of velocity in the range direction appears shifted, so it appears to be travelling not along the railway track, but displaced to the side! As another example, a ship in a satellite SAR image with a radial velocity of 10 m/s at a range of 1,200 km would experience an azimuth shift of 1.7 km. On the other hand, the ship wake (which is stationary) appears in the correct position. Thus the ship appears not at the tip of the wake, but displaced in azimuth. This effect is visible in a number of space-borne SAR images. From the knowledge of the geometry, and of the azimuth shift, it is possible to estimate the target velocity.

4. PROCESSING SCHEMES

In the following several processing schemes for detection and imaging of moving target are described.

4.1 MTI+PD

The material of this Section is derived by [DDB94] that describes the work done by Colleagues of the Author. The processing technique, referred to as moving target detection and imaging (MTDI), has been derived by the well known moving target detection (MTD) processing widely used in conventional ground-based radars. A range-Doppler SAR processing is adopted; the raw data are firstly processed along the range direction and then along the azimuth. An azimuth processor is developed to detect the presence of a moving point like target in

each range cell and to measure its velocity components. The method is valid under the following hypotheses, namely:

- the target velocity is bounded within a minimum detectable and a maximum unambiguous values, and
- the SAR system and the moving target cause a negligible range migration.

The mathematical model of the echo received by the radar antenna during the synthetic aperture time interval is reported in this section. Fig. 2 sketches the geometry of a SAR system and a moving object of interest. The antenna, on board of an aircraft, moves along the azimuth direction x . The antenna beam pattern is directed orthogonal to the flight path; θ (the off-nadir angle) is the angle formed by the normal to the ground and the line from the radar to the central point of the scene; v_x and v_y are the velocity components of the target along the reference coordinates. Along the azimuth, the radar transmits pulse trains with repetition frequency, PRF, each pulse having a linear frequency modulation (chirp). To account for some unpredictable changes in the environment wherein the transmitter operates, an unknown initial phase ϕ_0 , modeled as a random variate uniformly distributed in $(0, 2\pi)$ is assumed in the transmitted signal. At the n th azimuth position of the antenna, the transmitted pulse is expressed as

$$T_n(t) = A \cos(2\pi f_0 t + \alpha t^2 + \phi_0), \quad -\tau/2 \leq t \leq \tau/2 \quad (3)$$

where:

- A and τ are the pulse amplitude and the pulse width, respectively,
- f_0 is the carrier frequency,
- $\alpha = 2\pi B/\tau$ is the chirp rate, and
- B is the chirp bandwidth.

Consider now a point-like scatterer on a completely absorbing background; the echo received by the antenna at the n th azimuth position, after down frequency conversion, can be modeled as

$$S_n(t) = A l \sigma_0 g_0(\theta, \varphi) \exp(j\alpha(t-t_d)^2) \exp(j4\pi R_n/\lambda + \phi_0) + \eta(t-t_d) \quad (4)$$

where:

- σ_0 is the complex reflection coefficient of the scattering point,
- $g_0(\theta, \varphi)$ is the antenna gain evaluated at the angular coordinates θ and φ of the target,
- $R(t)$ is the radar-target range and $R_n = R(t_n) = R(n/\text{PRF})$,
- l is the attenuation factor accounting for propagation losses,
- $t_d = 2R_n/c$ is the time delay due to the two-way path,
- λ is the wavelength, and
- $\eta(t)$ is the system noise.

The relative radar-target motion induces a Doppler modulation on the signal received along the azimuth direction: it is a linear frequency modulation (azimuth chirp), characterized by two parameters, a frequency shift (Doppler centroid) and a frequency rate (Doppler rate). For narrow azimuth beam width, the expressions for the Doppler centroid and the Doppler rate are

$$F_{dc} = \frac{2v_y \sin \theta}{\lambda} \quad (5)$$

$$F_{dr} = \frac{2(V - v_x)^2}{\lambda R_0} \quad (6)$$

where V is the platform speed and R_0 is the range between the platform and the scene center. The above approximation leads to a useful expression for the bandwidth of the azimuth chirp, i.e.

$$B_d = \frac{2(V - v_x)}{L} = F_{dr} T_i \quad (7)$$

with L being the along-track antenna length and T_i the integration time, i.e. the time during which the target is illuminated by the antenna main lobe. The signal $S_n(t)$, sampled at the proper frequency F_c , is stored as a column in the holographic matrix Ξ . The dimensions, N_{sr} and N_{sa} , of the matrix Ξ represent the number of range and the azimuth samples, respectively. The entry S_{mn} of Ξ can be re-parameterized to elicit the dependence on the Doppler centroid F_{dc} and the Doppler rate F_{dr} , namely

$$S_{mn} = A I \sigma_0 g_0(\vartheta, \varphi) \exp(j\alpha(t_m - t_d)^2) \cdot \exp(j2\pi(F_{dr} t_n^2 + F_{dc} t_n)) \exp(j\phi_0) + \eta(t_m - t_d) \quad (8)$$

where $t_m = m/F_c$ is the range time (fast time) and t_n is the azimuth time (slow time). A conventional SAR processor, designed to provide the image of a stationary scene, works separately along the range and the azimuth directions. Specifically, at the first stage each column of the holographic matrix is convolved with the impulse response function (IRF) h_r of the range filter yielding the range-compressed data. At the second stage, each row of the resulting matrix is convolved with the IRF h_a of the azimuth filter, thus providing the final image. Useful expressions for h_r and h_a , derived from (8), are

$$h_r(t_m) = \exp(j\alpha t_m^2), \quad m = 1, 2, \dots, N_t \quad (9)$$

$$h_a(t_n) = \exp(j2\pi F_{dr0} t_n^2), \quad n = 1, 2, \dots, N_a \quad (10)$$

where F_{dr0} is the Doppler rate (6) for $v_x=0$. The conventional processing fails when the convolutions are implemented by means of (9) and (10) on the signals coming from moving objects for which $F_{dr} \neq F_{dr0}$ and $F_{dc} \neq 0$.

In MTD technique the Doppler frequency shift is used as a means of detecting moving targets embedded in a strong ground backscatter (clutter). A delay-time canceller behaves as a filter to reject the low Doppler components associated with the clutter and to preserve the high Doppler components of the moving targets. The canceller is cascaded with a bank of narrow-band filters (channels), uniformly spread in the PRF interval. When matched filtering is performed, only that Doppler channel containing the target echo will supply a significantly nonzero output. These concepts are amenable to extension to SAR application: in fact, for sensing and imaging purposes, the stationary scene resembles clutter and the point-like moving object represents the target. It appears convenient to refer to this approach as MTDI, since it is the natural extension of MTD to SAR. However, some novel problems, arise when we deal with SAR. First, the representation of the signal returned by a scatterer results in an intrinsically two-dimensional problem. In the airborne case, however, the dwell-time is usually short and the range cell migration is avoided. Whenever the SAR system parameters do not induce range migration by themselves, a moving target could be still displaced over more range lines if its radial velocity is high enough to encompass more range lines during the integration time, i.e. if

$$N_{rcm} = \frac{v_y \sin \theta T_i}{\delta_r} > 1 \quad (11)$$

where N_{rcm} is the number of range migration cells and δ_r is the range resolution of the SAR system. Assuming an airborne SAR operating at millimetric wavelengths (for example $T_i=0.2s$, $\theta=45^\circ$, $\delta_r=4$ m), and substituting the numerical values in (11), a maximum target speed of 30 m/s along the range direction is allowed to avoid range migration ($N_{rcm}<1$). Under these assumptions the pattern is not truly bi-dimensional and the processing can be performed by a separate filtering of the rows and the columns of the holographic matrix. Another

problem which arises when dealing with moving targets is the aliasing effect due to the broadening and shifting of the signal spectrum. Assume, in fact, that $PRF = B_d$: in this case a radial velocity component of the target causes a Doppler shift according to (5) and a significant aliasing cannot be avoided. Furthermore, if the target velocity v_x is opposite to that of the platform, an increase of the nominal bandwidth occurs according to (7). As a consequence of these concurrent phenomena, the azimuth compression cannot be perfectly achieved and the target is not correctly imaged. If instead the sampling frequency PRF complies with the Nyquist theorem (that is, for example, if $PRF \gg B_d$), then the discrete and the analogue representations can be considered equivalent. More precisely, the PRF must be constrained by the inequality

$$PRF \geq 2[F_{d_{\max}} + (T/2)F_{dr_{\max}}] \quad (12)$$

where $F_{d_{\max}}$ and $F_{dr_{\max}}$ are available from (6) and (5) on substituting the quantities v_x and v_y with their maximum values. The basic considerations leading to the MTDI algorithm as a means of detecting moving targets are discussed below. When the system PRF complies with Eq. (12), the ground echo and the echoes of the moving targets are spectrally separated: the former is concentrated in $[-B_d/2, B_d/2]$ and the latter are allocated in $(-PRF/2, -B_d/2) \cup (B_d/2, PRF/2)$.

The scheme of the MTDI processor is shown in Fig. 3. The raw data are stored in the holographic matrix and fed into the range processor. Then, the spectrum of the azimuth line is computed via a fast Fourier transform (FFT) and split throughout the N_{dc} channels, each one encompassing a bandwidth as large as B_d . The rejection of the ground echo is performed leaving out the channel centered on the zero Doppler frequency, after phase compensation of the platform speed V . The processing that follows performs azimuth compression on each stream of data. The procedure consists in evaluating the product between the data coming from a single channel and a suitable reference function, making an inverse Fourier transform and comparing the maximum value attained by the signal with a threshold. Finally, if a moving point is detected, a fine estimate of the chirp parameters – as discussed in [DDB94] – is provided to improve the performance of the imaging forming algorithm. The range of detectable velocities is limited between a minimum detectable and a maximum unambiguous values. The minimum and maximum velocities correspond to a Doppler displacement equal to the first and the last available Doppler channel center frequencies, respectively. Conservative values (with respect to the off-nadir angle) are

$$v_{\min} = \frac{\lambda B_d}{2} = \frac{\lambda V}{L} \quad (13)$$

$$v_{\max} = \frac{\lambda}{4}(PRF - B_d) \quad (14)$$

For airborne SAR's operating at millimetric wavelengths, values of 1 m/s for v_{\min} and 20 m/s for v_{\max} are found using a PRF of 10 kHz.

In [DDB94] the problem of probing the presence of a chirp signal embedded in a disturbance environment (backscattering by fixed scene and thermal noise) is modeled as a binary decision test; also the detection performance are found. Details are in the quoted reference.

A high quality image of moving targets calls for suitable procedures for estimating the chirp parameters. Here we introduce two algorithms for Doppler centroid and Doppler rate estimation. The algorithms are suited for airborne SARs and point-like targets. The chirp parameters are related to the moving point velocities through (5) and (6), the knowledge of the former allows one to recover the latter.

Doppler centroid estimate. The target radial velocity causes a Doppler frequency shift given by (5). The algorithm discussed here involves a correlation between the power spectrum of the azimuth signal and that of a reference signal, namely a chirp signal with no Doppler shift and nominal Doppler rate. The correlation peak is centered on the searched Doppler shift. More formally, the algorithm consists of the following steps

- Discrete Fourier transformation (DFT) of the azimuth signal,

$$X(m) = \sum_{n=0}^{N_{ba}-1} x(n) e^{-j2\pi mn / N_{ba}} \quad (15)$$

where N_{ba} is the azimuth FFT block length, and computation of the power spectrum,

$$S_x(m) = |X(m)|^2 \quad (16)$$

- Extraction of a subset of samples $S(m)$ from $S_x(m)$ according to the following rule: once the channel where detection occurs is selected, pick up all samples encompassing a bandwidth as large as $2B_d$ centered around the channel reference frequency. So we are ensured that only a small amount of the signal energy is left.
- Evaluation of the cross-correlation $R_s(m)$ between $S(m)$ and reference spectrum $S_r(m)$

$$R_s(m) = S(m) \otimes S_r(-m) \quad (17)$$

where denotes \otimes convolution.

- When the point-like target moves along v_x , a mismatch occurs between the signal and the reference spectra. As a consequence, the cross-correlation function no longer produces a sharp peak. However, a good accuracy can still be provided using an energy balancing algorithm. Thus, define

$$\begin{aligned} \epsilon_1 &= \sum_{\Omega_1} \bar{R}_s(m) \\ \epsilon_2 &= \sum_{\Omega_2} \bar{R}_s(m) \end{aligned} \quad (18)$$

where Ω_1 indicates the set of samples belonging to the lower frequencies ($m=1, \dots, n_1$, say) and Ω_2 indicates the corresponding set belonging to the upper frequencies ($m=n_1+1, \dots, n_p$, say) (n_p is the total number of points of $R_s(m)$). We select n_1 so that the difference $|\epsilon_1 - \epsilon_2|$ is minimum. The knowledge of n_1 can be used for the evaluation of the Doppler centroid.

Airborne SAR autofocus. The Doppler rate is the other parameter required to perform a sharp focusing of the target echo. A widely used algorithm for Doppler rate estimation is based on the multi-look technique; unfortunately, this technique does not work well if applied to airborne SAR's. Consider, in fact, the Doppler rate resolution achievable by this algorithm [DDB94]

$$\delta F_{dr} = \frac{F_{dr0}^2}{F_{dr0} + \Delta f \frac{B_d}{N_L}} \quad (19)$$

where: N_L is the number of looks, Δf is the center-looks distance. Table 1 reports the values assumed by the above-specified parameters, together with the Doppler resolution, for typical space-borne and airborne SAR systems. It is easy to observe that the resolution is good for Seasat SAR but poor for the airborne SAR. In [DDB94] a new algorithm is introduced which performs an accurate estimation of the Doppler rate for both

space-borne and airborne SAR's provided that the Doppler centroid has been previously corrected. Consider the modulus of the mutual energy ε between the received signal $x(t)$ and the signal $x_r(t)$

$$|\varepsilon(\beta)| = \frac{1}{T_1} \left| \int_{-T_1/2}^{T_1/2} x(t, F_{dr}) x_r^*(t, \beta) dt \right| \quad (20)$$

where β is the Doppler rate to be estimated. The received chirp $x(t, \beta)$, after Doppler centroid correction, can be simply expressed as

$$X(t, F_{dr}) \cong \exp \{ j F_{dr} t^2 \} \quad (21)$$

If we choose

$$x_r(t, \beta) = \exp \{ j \beta t^2 \} \quad (22)$$

and collect all inessential terms in a complex constant K , we obtain

$$|\varepsilon(\beta)| = \left| K \int_{-T_1/2}^{T_1/2} e^{j(F_{dr} - \beta)t^2} dt \right| \quad (23)$$

which can be approximated as

$$|\varepsilon(\beta)| = \left| K \sum_{k=N_p/2}^{N_p/2-1} \exp \{ j[(F_{dr} - \beta)t_k^2] \} \right| \quad (24)$$

Expression (24) can be regarded as the integration of N_p pulses having the same modulus, but time varying phase. The integration process leads to the maximization of the cross-energy modulus if and only if $(F_{dr} - \beta)$ is equal to zero or, in other words, if the estimated Doppler rate is equal to the true one. Thus, the estimation rule amounts to evaluating the maximum of expression (24), with respect to β , namely

$$\hat{\beta} = \max_{\beta \in \Omega_\beta} |\varepsilon(\beta)| \quad (25)$$

where Ω_β is a suited domain for β .

After the estimation of F_{dc} and F_{dr} , the azimuth signal can be correctly compressed by means of a classical SAR azimuth processing to obtain the position and the reflectivity of targets. Moreover, v_x and v_y can be evaluated by applying Eqs. (5) and (6). The algorithms above have been simulated to check their ability to generate correctly focused images of moving and stationary point-like targets over a fixed background; the successful results are reported in [DDB94].

Table 1

	Seasat SAR	Airborne SAR
f_{dr0}	520 Hz/s	3112 Hz/s
Δf	967 Hz	300 Hz
B_d	1389 Hz	400 Hz
N_L	4	4
δf_{dr}	0.8 Hz/s	292 Hz/s

4.2 ALONG TRACK INTERFEROMETRY (ATI) – SAR

In a similar manner to DPCA (see Section 4.3), along-track interferometry (ATI) uses two displaced antennas connected to two receiving channels. For each channel a SAR image can be generated. The time delay between the azimuth signals can be compensated during the azimuth compression using two different reference signals, incorporating the azimuth chirps generated in the two channels by a common point scatterer. If the first image is multiplied by the complex conjugate of the second, the remaining phase is zero for stationary objects and non-zero otherwise. If the two receivers are spatially separated by the distance d , the interferometric phase is approximated by $\varphi = -(2\pi/\lambda)d(v_r/v_a)$, where v_r is the radial velocity of the target.

An example of parameters for ATI SAR is: $d = 1m$, $v_a = 100m/s$, $\lambda = 3cm$, $v_r = 1m/s$, $\varphi = 120^\circ$. ATI-SAR was originally developed to measure the speed ocean surfaces; in [END99] the capability of SAR to detect slowly moving targets is shown on live data. In [GIE02] an in-depth analysis of the capabilities of ATI-SAR to detect moving targets is presented. In this section some analytical and simulation results concerning detection of moving target is presented. ATI-SAR has the following limitation: to have a high phase sensitivity, the two antennas have to be widely separated, but this leads to a comb of blind velocities $v_{blind} = kv_a\lambda/d$, where k is an integer: this limits the useful target velocity interval; moreover, the above mentioned distortions in the SAR image of moving target (Section 3) remain.

The probability density function (pdf) of the interferogram phase φ for just stationary clutter and thermal noise has been found to be [LHM94].

$$p(\varphi) = \frac{1}{2\pi} \frac{1 - |\gamma|^2}{|\gamma|^2 \cos^2 \varphi} \left\{ 1 + \frac{|\gamma| \cos \varphi \cdot \cos^{-1} [|\gamma| \cos \varphi]}{[1 - |\gamma|^2 \cos^2 \varphi]^{0.5}} \right\}$$

where

$$\gamma = \frac{E\{i_1 i_2^*\}}{(E\{|i_1|^2\} E\{|i_2|^2\})^{0.5}} \quad (26)$$

$$\gamma = \frac{\gamma_c}{1 + 1/CNR}$$

Clutter and noise are independent random processes with zero mean and Gaussian pdf. Radar echoes i_1, i_2 received by the two antennas at the same time have a correlation coefficient γ which depends on the endogenous correlation coefficient of clutter γ_c and the clutter-to-noise power ratio $CNR = P_c/P_n$: thus the presence of noise reduces the clutter coherence. In practice, the interferometric phase is estimated by averaging n looks as follows

$$\varphi = \arg \left(\frac{1}{n} \sum_{k=1}^n i_1(k) i_2^*(k) \right) \quad (27)$$

The corresponding pdf becomes

$$p(\varphi) = \frac{\Gamma(n+1/2)(1-|\gamma|^2)^n \beta}{2\sqrt{\pi} \cdot \Gamma(n)(1-\beta^2)^{n+1/2}} + \frac{(1-|\gamma|^2)^n}{2\pi} {}_2F_1(n, 1; 1/2; \beta^2)$$

$$\pi < \varphi \leq \pi \quad (28)$$

$$\beta = |\gamma| \cos \varphi$$

where ${}_2F_1(\bullet)$ denotes the Gaussian hypergeometric function. For $n=1$ (28) reduces to (26). Recently a mathematical expression of the pdf has been presented in [GIE02] also for the case of target presence. In the following we illustrate some simulation results concerning the pdf of interferogram in presence of target, clutter and noise.

The mathematical expression (28) plays an important role in finding the detection threshold for a prescribed value of false alarm probability (P_{fa}). By numerical integration the following numerical values for the threshold Th have been found.

$\gamma = 0.9 \rightarrow Th = 1.0505$; $\gamma = 0.98 \rightarrow Th = 0.3802$; $\gamma = 0.99 \rightarrow Th = 0.2301$; the prescribed false alarm probability, the clutter - to- noise power value and the number of averaged looks are: $P_{fa} = 10^{-4}$, $CNR = 20dB$, $n = 4$. The variation of the detection threshold with the number of averaged looks for $CNR = 20$ dB, $\gamma = 0.98$ and $P_{fa} = 10^{-4}$ is as follows:

$$n = 1 \rightarrow Th = 2.8414; n = 2 \rightarrow Th = 0.9505; n = 4 \rightarrow Th = 0.3802;$$

$$n = 6 \rightarrow Th = 0.3002; n = 10 \rightarrow Th = 0.2201.$$

The target has been modeled as Swerling 1. Figure 4 depicts the histogram of phase interferogram for the following parameters: two antennas, $n = 4$, clutter Doppler phase = 0, $CNR = 20$ dB, $\gamma = 0.98$, target Doppler phase: $\varphi_{target} = 1.3rad$. It is noted that when the signal-to-clutter power ratio (SCR) is very small in dB, the histogram coincides with the one predicted by equation (28); with the increase of the SCR the peak of the interferogram migrates on the target Doppler phase. Figure 5 illustrates the contour curves with constant detection probability versus target Doppler phase and SCR. The relevant parameters are: two antennas, $CNR = 20$ dB, number of averaged looks $n = 4$, correlation coefficient: $\gamma = 0.98$, $P_{fa} = 10^{-4}$ (detection threshold = 0.3802 rad). The following comments are in order: the contour curves are aliased in the interval $\varphi = [-\pi, \pi]$; detection is practically zero for low values of the target Doppler phase because of the numerical value of the detection threshold; the detection increases with the increase of the SCR value.

Next areas of research are in the field of removal of aliasing by using different values of carrier frequency [PSF01a]. In [PSF00], [PSF01] the possibility to do ATI-SAR with one bit coded SAR signal is demonstrated for moving target detection: this is another lively area of research; it has a bonus in terms of simplicity of processing implementation.

4.3 DPCA

The concept of DPCA: Displaced Phase Center Antenna was conceived by F. R. Dickey, F. M. Staudaher, and M. Labitt; in 1991 they received the IEEE-AESS Pioneer award for this invention [DSL91]. One major application of DPCA is in the JSTARS (Joint Strategic Target Attack Radar Systems) [SHN94]. Figure 6 shows the working principle of the system; it depicts the radar antenna moving along track when two pulses are transmitted and corresponding echoes received. The antenna is divided in two sub-arrays; the whole

antenna transmits two successive pulses, the corresponding echo of the 1st pulse is received by the fore sub-array, the echo of the 2nd pulse is received by the aft sub-array. Due to the aircraft movement, the transmitting and receiving antennas form two bistatic configurations for the two pulses. However, if the antenna dimension, the platform speed and the radar PRF are properly selected, the phase center of the bistatic antenna configuration for the 1st transmitted-received pulse coincides with the phase center of the 2nd transmitted-received pulse. Thus, the clutter is seen at two different time instants from a same radar location: the platform motion has been compensated, consequently the Doppler spectrum of clutter is not spread due to platform motion: The clutter is cancelled by subtracting the echoes of the 1st pulse received by the fore sub-array from the echo of the 2nd pulse received by the aft sub-array; DPCA corresponds to a kind of spatial MTI. Stationary targets should cancel, but echoes from moving targets will give a non-zero result from the subtraction, so they should remain. Coe and White [CWH96] have carried out a theoretical and practical evaluation of this technique. They have found that cancellation of the order of 25 dB is possible. The major DPCA sources of limitations are: loss of receiving aperture, PRF-velocity constraint, performance limited by sub-array mismatch of radiation patterns, two degrees of freedom (DOFs) only, the system is not adaptive. STAP is the natural generalisation of DPCA, in fact it has the following features:

- generalisation of adaptive array of antennas for jammer nulling,
- generalisation of DPCA for clutter cancellation,
- freedom in shaping the null,
- less constraints on the spacing of the antenna elements,
- compensation of platform motion along (as DPCA) and orthogonal to the array thus avoiding clutter spectral spreading.

4.4 SPACE-TIME-FREQUENCY

In this section a method for detecting and imaging objects moving on the ground and observed by a SAR is described. The method is based on the combination of two processing steps: 1) space-time processing which exploits the motion of an antenna array for canceling the echo from background, and 2) time-frequency processing which exploits the difference in time allocation of the instantaneous spectrum corresponding to echoes from the ground or from moving objects, for an adaptive time-varying filtering and for the estimation of target echo instantaneous frequency, necessary for producing a focused image of it. The design and performance of the space-time filter is described in [BFA90], [BFA91], [BFA92], [BFA94]. Some of the theoretical aspects of STAP of interest for this paper are discussed also in a number of publications; [LOM96c] discusses the optimum processing scheme for a special case and an approximation of it realised with a two-dimensional FIR (Finite Impulse Response) filter. Other relevant references are: [FAT92], [LFA96] and [LOM98]. Here we concentrate on the time-frequency step (Section 4.4.1) and on the joint space-time-frequency (Section 4.4.2).

4.4.1 Joint time-frequency analysis by Wigner-Ville distribution

The aim of this section is to show how time-frequency representation by WVD of the echoes received by a SAR provides a useful tool for detection of moving objects and estimation of instantaneous phase shift induced by relative radar-object motion [BFA92]. The phase history is then used to compensate the received signal and to form a synthetic aperture with respect to the moving object, necessary to produce a high resolution image. A method for extracting the instantaneous phase is based on the time-frequency (TF) distribution of received signal. The WVD has been chosen here because it presents some important features concerning detection and estimation issues. There are simple methods for analyzing signals in the TF domain, such as the short-time Fourier transform (STFT), but they do not exhibit the same resolution capabilities in the TF domain as does the WVD. In particular, since the STFT is based on a Fourier transform (FT) applied to a time windowed version of the signal, with the window central instant varying with time, the frequency resolution is inversely proportional to the window duration. The narrower the window, the better is the time resolution, but the worse is the frequency resolution and vice versa. Conversely, the WVD does not suffer from this shortcoming. The

WVD provides a higher concentration of signal energy in the TF plane, around the curve of signal instantaneous frequency (IF). This allows a better estimation of IF in presence of noise and this information is exploited for the synthesis of the long aperture with respect to moving object. On the other hand, the WVD poses other problems since it is not a linear transformation. This causes the appearance of undesired cross-products when more than one signal is present. Mapping of the received signal in TF plane provides a tool for synthesis of the optimal receiver filter without a-priori knowledge of the useful signal, provided that the signal-to-noise ratio be sufficiently large. The TF representation provides a unique tool for exploiting one of the most relevant differences between useful signals and disturbances in the imaging of small moving objects, namely the instantaneous frequency and the bandwidth. In fact, it can be shown that, while the bandwidth occupied by a target echo during the observation interval necessary to form the synthetic aperture mainly depends on radar-object motion, the instantaneous bandwidth is proportional to object size. Therefore the echo corresponding to a small target can occupy a large band during the overall observation time, but its instantaneous bandwidth is considerably narrower (i.e. the echo back-scattered by a point-like target has zero instantaneous bandwidth but it may exhibit a large overall bandwidth). Conversely, the echo from the background and the receiver noise have a large instantaneous bandwidth. Therefore, even if the useful signal and the disturbance may have a large total band, the possibility of tracking the instantaneous bandwidth, made available by the TF representation allows a discrimination of the useful signal from the disturbance not possible by conventional processing. Another important and unique advantage related to use of the WVD is that it allows the recovery of the echo phase history even in the case of undersampling, as shown in [BAR91]. This is particularly important in SAR applications since it allows us to work with PRF lower than the limits imposed by the signal bandwidth occupied during the observation interval. Owing to the target motion, this bandwidth may be considerably larger than the bandwidth occupied by the background echo. According to conventional processing, we should then use a correspondingly higher PRF. Conversely, if the useful signal has a large total bandwidth, but a narrow instantaneous bandwidth, the TF representation prevents superposition of spectrum replicas created by undersampling because, even if the replicas occupy the same bandwidth, they occur a different times. This property allows us to recover the desired information even from undersampled signals. Since the PRF value imposes a limit on the size of the monitored area, due to time - and then range - ambiguities, the possibility of using a low PRF prevents the reduction of the region to be imaged, as well as the increase of the data rate.

The WVD of a signal is defined as:

$$W(t, f) = \int_{-\infty}^{+\infty} s\left(t + \frac{\tau}{2}\right) s^*\left(t - \frac{\tau}{2}\right) \exp(-j2\pi f\tau) d\tau \quad (29)$$

where $s(t)$ represents the analytic signal. The estimation of the instantaneous frequency of signal is done as follows. Express the signal in terms of its envelope and phase

$$s(t) = a(t) \exp \{j\varphi(t)\} \quad (30)$$

It can be shown that the local or mean conditional frequency of the WVD distribution, defined as

$$\langle f \rangle_t = \left\{ \int_{-\infty}^{+\infty} f W(t, f) df \right\} \left\{ \int_{-\infty}^{+\infty} W(t, f) df \right\}^{-1} \quad (31)$$

is equal to the signal IF

$$\langle f \rangle_t = \frac{1}{2\pi} \frac{d\varphi(t)}{dt} \quad (32)$$

The estimate of the mean conditional frequency of the WVD then provides the information about the signal IF. This is exactly the information we need for re-phasing the received signal in order to produce a focused image.

Explain now the rationale for using the WVD to detect a moving target and estimate its parameters with SAR data. The received signal is the sum of echo from the moving object, whose phase modulation is unknown, plus clutter (the echo from fixed background), plus noise. The echoes from the fixed scene represent, in our case, a disturbance. The aim is to detect the presence of moving objects and to estimate their motion parameters. The detection and parameter estimation performance depend on the signal-to-clutter power ratio (SCR). If this ratio is small, we have to process first the received signal, in order to improve it as much as possible. This operation can be carried out by matched filtering. However, the matched filter can be defined only if the shape of the useful signal is known, and this is not the case. It turns out that the two operations, detection and parameter estimation, cannot be separated: estimation of the useful signal parameters can be carried out only after having detected the presence of a useful signal; a reliable detection, on the other hand, requires the knowledge of the signal parameters, in order to carry out a proper matched filtering, before the detection itself. It is then necessary to carry on these two kinds of operations contemporaneously. The time-frequency analysis of the received signal, in particular the WVD, provides a powerful tool for achieving the aforementioned requirements and extracting the desired information, namely the energy and the phase history. These two information are what we need for our purposes: the detection of the presence of a moving target is made by comparing the energy with a suitable threshold; the instantaneous phase is used to phase-compensate the received signal, for a correct coherent integration, necessary to imaging purposes. As regards the effect of disturbances in the received signal, it is useful to recall that matched filtering can always be performed by cascading: a clutter cancellation followed by a coherent integration. The first operation does not require knowledge of the useful signal shape, whereas the second operation does. In particular, a correct coherent integration requires knowledge of the signal phase history. The time-frequency analysis aims to facilitate extraction of the signal phase history. Therefore, the sequence of operations to be performed on the received signals is the following: a clutter cancellation is performed first and the output of the cancellation filter is analyzed in the TF domain. If the clutter has been reduced to a power level sufficiently smaller than the useful signal, the parameters estimated by the WVD are correct, within an error depending on the achieved SCR. These parameters provide the information necessary to set up a correct coherent integration. This rather intuitive reasoning for using the WVD in detection and estimation problems is formalized into the framework of the matched filter theory in [BFA92]; here we give a summary of main results concerning the application to SAR problem.

The signal received by a SAR is given by the sum of the echoes from the ground, the echoes from a possible moving object and receiver thermal noise. The echo from the ground can be modelled as a correlated random process, whose power spectral density is proportional to the antenna power radiation pattern. The echo from a moving object is characterised by an unknown modulation, induced by the relative motion between the radar and the object. In SAR imaging, we are interested in the phase modulation induced by the relative radar-target motion. If the transmitted signal is

$$p(t) = a(t) \exp(j2\pi f_0 t) \quad (33)$$

where $a(t)$ is the analytic signal and f_0 is the carrier frequency, the echo received by a point-like scatterer at a distance $r(t)$ from the radar is proportional to

$$p\left(t - \frac{2r(t)}{c}\right) = a\left(t - \frac{2r(t)}{c}\right) \exp(j2\pi f_0 t) \exp\left(j\frac{4\pi}{\lambda} r(t)\right) \quad (34)$$

During the observation interval, the amplitude of each backscattering coefficient can be assumed constant since the aspect angle does not vary by an amount such as to justify a change in the reflectivity characteristics (this assumption underlies all SAR signal processing). The only modulation of interest then is phase modulation. In the formation of the synthetic aperture, we are interested in the last term of the expression

above. The conventional techniques for autofocusing extended scenes compensate only linear and quadratic phase shifts. This means that only slow fluctuations (with respect to the integration time) are compensated. Conversely, the TF approach allows estimation and compensation of any kind of phase history. The distance $r(t)$ can be modelled as the sum of slow and rapid fluctuations, with respect to the observation interval. Slow variations can be expressed as a low-order polynomial, whereas fast variations follows a sinusoidal behavior, whose period is shorter than the time observation interval. The change in the distance causes a phase modulation, which must be compensated to obtain a correct image. The variation of distance can cause migration of the received echo over different range cells, depending on the ratio between the amount of variation and the range resolution. The range migration problem can be faced according to the double-resolution strategy outlined in the next Section 4.4.2. According to the strategy, all the phase estimations are carried out on data whose range resolution is such as to consider the migration negligible. According to the formulation of matched filtering in terms of the WVD, the processing scheme for detecting and estimating the parameters of the echoes from moving objects is sketched in Fig. 7. The received signal is first range-compressed. Then it is processed by a moving target indicator (MTI) filter to reduce the clutter contribution; in Section 4.4.2 we explain how to use STAP. The analysis of the signal in the TF domain allows estimation of the signal instantaneous frequency. Some smoothing can be applied on the WVD to improve the estimation accuracy. The instantaneous frequency is then integrated to obtain the phase modulation to be used for phase compensation of the received signal. At this point an FFT is sufficient to provide the high cross-range resolution image. A threshold is then applied to the envelope signal to check for detection. An example of an image relative to a moving point-like target superimposed on a fixed extended scene is reported in [BFA92]; the simulation results convey a positive feeling on the performance of the processing scheme of Figure 7.

4.4.2 Joint space-time-frequency analysis

The space-time and the time-frequency processing can be combined to form a processor that allows both the cancellation of the clutter echoes and the compensation of the target motion, necessary for the formation of a high cross-range resolution image. The overall space-time frequency processing is shown in Figure 8. The echo from the ground is canceled by means of the space-time processing. Having canceled the background echo, we proceed to the estimation of the target instantaneous frequency which is done by resorting to the WVD. Before proceeding to the estimation, however, some care must be devoted to the range migration problem. In fact, the relative radar/target motion causes not only a phase shift, but also a range migration which cannot be neglected if it overcomes the range resolution. The radar echoes are sampled and arranged in a matrix, whose columns are relative to successive transmitted pulses and the entries of each column contain the echoes coming from different distances. Given a certain point, if its distance from the radar does not vary by an amount bigger than the size of a range resolution cell, the echoes from that point are all stored on one column. If all the points composing the observed scene satisfy this condition, no range migration occurs and the samples can be first processed in range, column by column, and then in cross-range, row by row. If, however, the echoes from some point occupy more than one row, the cross-range processing cannot be performed directly on the collected data, row by row. Some algorithm for compensating the range migration must be applied in order to realign the data, before the cross-range processing. Range migration compensation techniques have already been examined in the literature in the imaging of stationary scenes. The problem is harder in the imaging of moving targets, however, since the radar/target distance is not known. Two main problems arise when dealing with moving targets, in presence of range migration: 1) the migration causes a spreading of the target energy through many range cells, therefore the signal-to-noise ratio, for each range cell, decreases and this causes a loss of detectability, and 2) due to the lack of knowledge of the target range migration law, it is not known a priori which samples of the matrix of the collected data are to be taken for carrying out the estimation of the phase history.

Here we follow a two-step approach for compensating the migration problem: 1) a coarse range resolution, and 2) a fine range resolution analysis (see Figure 9). The rationale of the approach is based on the fact that the migration problem can be neglected if the amount of migration does not exceed the range resolution. Therefore, we can initially work in a low resolution mode, where the range resolution has been degraded by an

amount such as to make the migration negligible. A first detection is performed on these data: if a detection occurs, the processing chain for the estimation of the target echo phase history is enabled. The estimation is carried out in the time-frequency domain, according to the criterion described previously. Having once estimated the phase $\phi(t)$, we can evaluate the law of variation of the distance by exploiting the relationship between phase shift and distance

$$d(t) = \frac{\lambda}{4\pi} \phi(t) \quad (35)$$

By using $d(t)$, we can compensate for the range migration by properly rearranging the data in the matrix containing the received samples. These data can now be phase shifted to compensate for the phase shift induced by the target motion. The data undergo then a full range and cross-range compression for obtaining the high resolution image. The price paid by adopting the two-step resolution approach is the SNR loss inevitably related to the degradation of the range resolution in the coarse resolution mode. It is important to point out that, even if the cause of both phase shift and migration problems is the same, namely the variation of the radar/target distance, the phase shift is much more sensitive to range variation than the range migration. In fact, for example, in an X-band radar ($\lambda=3$ cm), having a range resolution of 1 m, an error on the distance of 7.5 mm causes a phase shift of π radians, while the corresponding range migration is absolutely irrelevant. This means that, having once estimated the phase history by the described procedure, the resulting value for the distance variation $d(t)$ is estimated with a good accuracy.

The performance of the space-time-frequency processing scheme has been evaluated by a simulation program which generates the echoes from an extended surface and from a point-like target and then applies the proposed algorithm [BFA94]. The target has been supposed moving on the terrain (shadowing effects have been neglected) at a constant velocity, in a direction oblique with respect to the radar motion. The velocity parameters have been chosen to make evident the presence of range migration and of cross-range smearing of the target image. The ground reflectivity has been assumed equal to the target reflectivity (this is a quite pessimistic assumption, because in many cases of practical interest, the target reflectivity is higher). The thermal noise, 40 dB below the target return, has also been assumed for the received signal. The ground echo is first canceled, by using a STAP with two-element antenna and two time samples. The two antennas are spaced by $d=vT$. A SAR image is then formed by conventional techniques. The result is shown in Fig. 14 of [BFA94]. The smearing of the moving point-like target is evident. Given the motion parameters, the target has migrated over six range cells. This is the cause for the broadening of the target image even in range, as well as in cross range. Anyway, the target echo causes a detection and initializes the motion estimation channel. The high resolution data are smoothed in range to decrease the range resolution. Then the processor looks for the range cell with the maximum energy content and computes the WVD of that cell only. The frequency history, and then the phase history, are evaluated, according to the procedure outlined previously. The phase history is then used for compensating the range migration and the phase shift on the high resolution range data. The final image is shown in Fig. 15 of [BFA94]. The sharpening of the target image is quite evident.

The method above corrects only the (translation) motion of a point-like target. If focused image of three-dimensional object is required, for recognition purposes, the motion parameters must be estimated to compensate correctly the relative signals ([WCJ90] and [FIE01]). Since the motion of any rigid body can be decomposed as the sum of the translation of a point plus the rotation of the other points around that point, in some cases, depending on the target dimension and kind of motion, the compensation of the only translation motion is not sufficient and we still have to compensate for the rotational motion. This second compensation can be efficiently performed in the frequency domain, by applying, for example, the method proposed in [WCJ90]. Algorithms have been conceived to produce fine resolution images of moving targets having any translation or rotation motions. They require the presence of multiple prominent points in the target image. The echo from a first point is initially analysed. Its phase is computed and subtracted pulse-to-pulse from the phase of the incoming signal. This operation removes the effect of the target translation motion and make this first point effectively the new center of the scene. At this point, if the rotational motion is negligible, conventional

SAR processing yields the focussed image. If, conversely, the rotation cannot be neglected, two other prominent points are required to estimate the rotation parameters. These parameters are used to compensate for the rotational motion in the frequency domain and help in applying the SAR processing correctly. The algorithm requires that the prominent points be separable and that their phases be estimated without interfering with each other. In some cases, however, this assumption might not be met: at high resolution, separability is more likely to occur, but the range migration could complicate the phase estimation problem; at low resolution, the range migration could be negligible, but it is more likely that some prominent points might occupy the same range resolution cell. Further analyses are necessary in the imaging of extended targets when more dominant scatterers occupy the same resolution cell. In this case, in fact, the bi-linearity of the WVD creates undesired cross-product terms which can seriously impair the estimation of the instantaneous frequency. A reduction of these undesired terms could be achieved by resorting to other time-frequency representations, such as the Choi-Williams distribution [COH89]. Another approach to contrast the appearance of undesired cross-product terms is described in [BZA92]. It is shown that it is still possible to estimate the signal parameters, even for multi-component chirp signals embedded in noise, by combining the WVD with the Hough transform.

5. CONCLUSIONS

In this paper processing techniques have been described to combine the SAR and STAP functions; the goal is to obtain a well focused target image in the right place on the image of the stationary scene. It has been shown that the three-dimensional processing in space- time and frequency gives good detection and imaging performance.

6. ACKNOWLEDGEMENTS

Moving target detection and imaging with SAR has been the subject of R&D work for a number of years in Selenia/Alenia (now AMS). The Author acknowledges with thanks the cooperation of a number of Colleagues; notably Professor S. Barbarossa (today with the University of Rome "La Sapienza") and Dr. E. D'Addio. More recently Dr. A. Gabrielli has cooperated in the development of ATI-SAR work.

7. REFERENCES

- [AUS84] D. Ausherman, A Kozma, J. Walker, H. Jones, E. Poggio, "Developments in radar imaging". IEEE Trans on Aerospace and Electronic Systems, July 1984, pp. 363-400.
- [BAR91] S., Barbarossa, "Parameter estimation of undersampled signals by Wigner-Ville analysis". IEEE International Conference on Acoustics, Speech and Signal Proc., ICASSP '91, Toronto, May, 1991, pp. 3253-3256.
- [BFA90] S. Barbarossa, A. Farina, "A novel procedure for detection and focusing moving objects with SAR based on the Wigner-Ville distribution". Proc. of IEEE Int. Radar Conf., Arlington, VA, May 7-10, 1990, pp. 44-50.
- [BFA91] S. Barbarossa, A. Farina, "Detection and imaging of moving objects with SAR by a joint space-time-frequency processing". Proc. of the Chinese International Conference on Radar, Beijing, China, October 22-24, 1991, pp. 307-311.
- [BFA92] S. Barbarossa, A. Farina, "Detection and imaging of moving objects with Synthetic Aperture Radar. Part 2: Joint time-frequency analysis by Wigner-Ville distribution". IEE Proc., Pt. F., Vol. 139, no. 1, February 1992, pp. 89-97.

- [BFA94] S. Barbarossa, A. Farina, "Space-time-frequency processing of synthetic aperture radar signals". IEEE Trans. on Aerospace and Electronic Systems, Vol. AES-30, no. 2, April 1994, pp. 341-358.
- [BZA92] S. Barbarossa, A. Zanalda, "A combined Wigner-Ville and Hough transform for cross terms suppression and optimal detection and parameter estimation". Proceedings of the IEEE International Conference on Acoustics, Speech and Signal Processing, ICASSP '92, Mar. 1992, San Francisco.
- [COH89] L. Cohen, "Time-frequency distributions - a review", Proc. IEEE, vol. 77, no. 7, 1989, pp. 941-981.
- [CWH96] D. J. Coe, R. G. White, "Experimental moving target detection results from a three-beam airborne SAR" Eusar 96, Konigswinter, Germany, 1996, pp. 419-422.
- [DDB94] E. D'Addio, M. Di Bisceglie, S. Bottalico, "Detection of moving objects with airborne SAR", Signal Processing, vol. 36, 1994, pp. 149-162.
- [DSL91] "IEEE AESS 1991 Awards to F. R. Dickey, F. M. Staudaher, M. Labitt", IEEE AES Magazine, May 1991, vol. 32, p. 32.
- [END99] J. H. G. Ender, "Space time processing for multichannel synthetic aperture radar", ECEJ Special Issue on STAP, Vol. 11, No.1, pp. 29-40, February 1999.
- [DFM89] E. D'Addio, A. Farina, C. Morabito, "Applications of multidimensional processing to radar systems". Invited paper. Proc. of International Conference on Radar, Versailles, France, pp. 62-78, 24-28 April, 1989.
- [FAT92] A. Farina, L. Timmoneri, "Space-time processing for AEW radar". Proc. of IEE Int. Conference on Radar 92, Brighton (UK), 12-13 October 1992, pp. 312-315.
- [FIE01] J. R. Fienup, "Detection of moving targets in SAR imagery by focusing". IEEE Trans. on Aerospace and Electronic Systems, Vol. AES-37, No. 3, pp. 794-809, July 2001.
- [FPO97] B. Friedlander, B. Porat, "VSAR- a high resolution radar system for detection of moving targets". IEE Proc. on Radar, Sonar and navigation, Vol. 144, No. 4, pp. 205-218, August 1997.
- [GIE02] C. Gierull, "Moving target detection with along-track SAR interferometry", DREO TR 2002-000, 09 January 2002.
- [KLE98] R. Klemm, "Space-time adaptive processing-principles and applications", IEE Publishers, 1998.
- [KLE99] Klemm R., "Introduction to space-time adaptive processing," *Electronics & Communication Engineering Journal*, Vol. 11, No. 1, pp. 5-13, February 1999.
- [LHM94] J.S. Lee, K. W. Hoppel, S. A. Mango, A. R. Miller, "Intensity and phase statistics of multilook polarimetric and interferometric SAR imagery", IEEE Trans on Geoscience and Remote Sensing, vol. No. 5, pp. 1017-1028, 1994.
- [LFA96] P. Lombardo, A. Farina, "Dual antenna baseline optimisation for SAR detection of moving targets". ICSP- International Conference on Signal Processing, Beijing (P. R. of China), 14-18 October 1996, pp. 431-434.

- [LOM96a] P. Lombardo, "Echoes covariance modelling for SAR along-track interferometry", IEEE Int. Symposium IGARSS '96, Lincoln, Nebraska (USA), May 1996, pp. 347-349.
- [LOM96b] P. Lombardo, "DPCA processing for SAR moving target detection in the presence of internal clutter motion and velocity mismatch", Microwave Sensing and Synthetic Aperture Radar, EUROPTO series, Vol. 2958, September 1996, Taormina (Italy), pp. 50-61.
- [LOM96c] P. Lombardo, "Optimum multichannel SAR detection of slowly moving targets in the presence of internal clutter motion", CIE-ICR '96, International Radar Conference Beijing, China, 8-11 Oct. 1996, pp. 321-325.
- [LOM98] P. Lombardo, "Data selection strategies for radar space time adaptive processing", 1998 IEEE Radar Conference, Radar'98, Dallas, Texas (USA), May 12-13, 1998.
- [LOM98a] P. Lombardo, "A Joint Domain Localized processor for SAR target detection", European Conference on Synthetic Aperture Radar, EUSAR'98, Friedrichshafen, Germany, 25-27 May 1998.
- [PSF00] V. Pascazio, G. Schirinzi, A. Farina, "Along track interferometry by one bit coded SAR signals", The EOS/SPIE Symposium on Remote Sensing, 25-29 September 2000, Barcellona, Spain.
- [PSF01] V. Pascazio, G. Schirinzi, A. Farina, "Moving target detection by along track interferometry", Proc. of IGARSS 2001, Sidney (Australia), July 2001.
- [PSF01a] V. Pascazio, G. Schirinzi, "Estimation of terrain elevation by multifrequency interferometric wide band SAR data", IEEE Signal Processing Letters, vol. 8, 2001, pp. 7-9.
- [SHN94] H. Shnitkin, "Joint STARS phased-array radar antenna", IEEE AES Magazine, October 1994, pp.34-41.
- [PDF99] R. Perry, R. Di Pietro, R. Fante "SAR imaging of moving targets", IEEE Trans. on Aerospace and Electronic Systems, Vol. AES-35, No. 1, pp. 188-200, January 1999.
- [WAR94] J. Ward, "Space-time adaptive processing for airborne radar", MIT Lincoln Laboratory, Technical report TR-1015, December 13, 1994.
- [WCJ90] S. Werness, W. Carrara, L. Joyce, And D. Franczak, "Moving target imaging algorithm for SAR data", IEEE Trans. on Aerospace and Electronic Systems, Vol AES-26, no. 1, pp. 57-67, 1990.

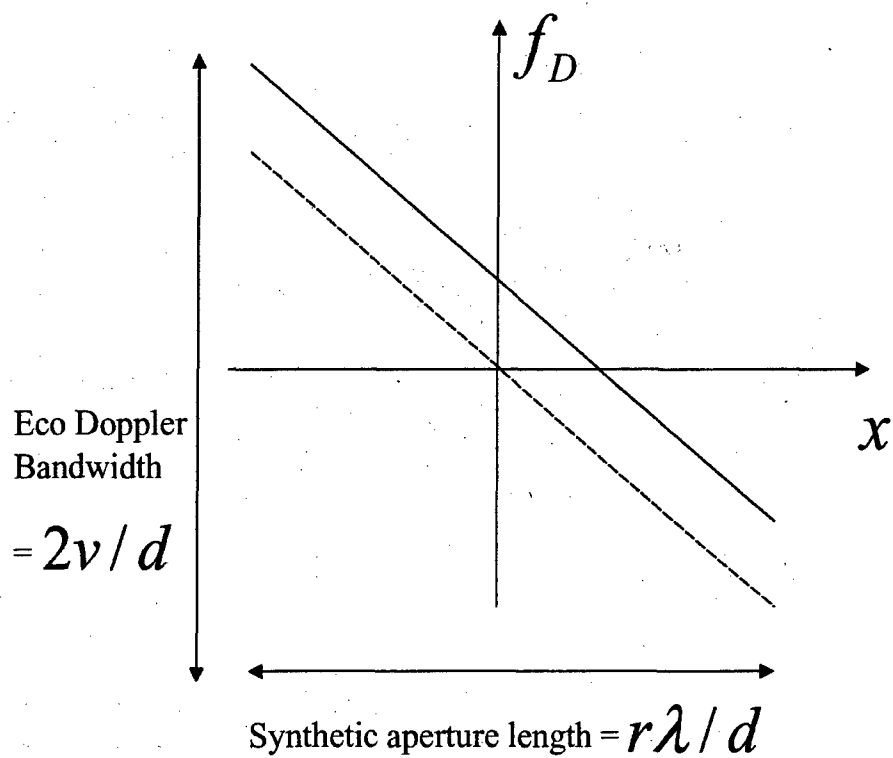


Figure 1: A target with a radial velocity is matched filter by the SAR processing thus producing a corresponding azimuth shift.

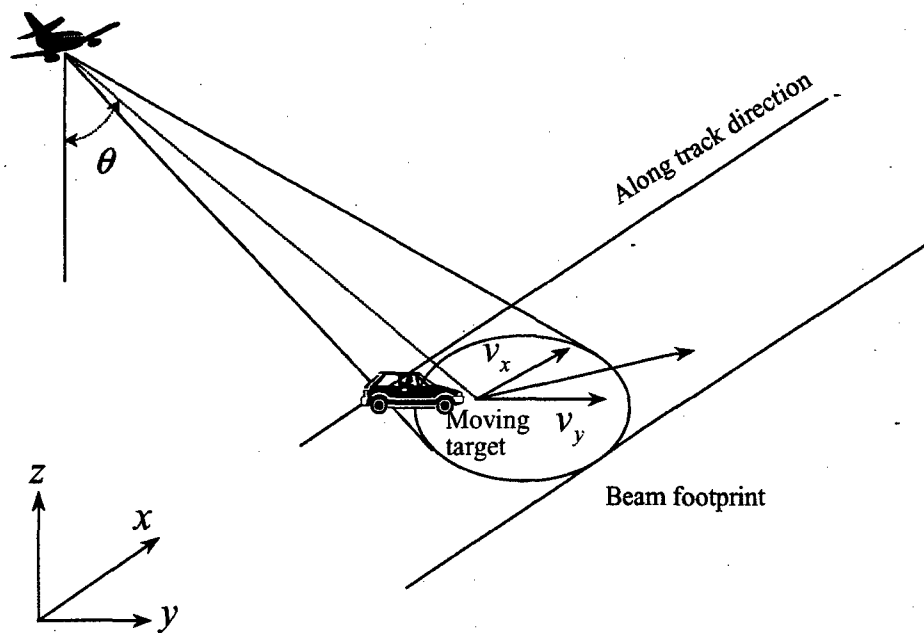


Figure 2: Geometry of SAR and moving target.

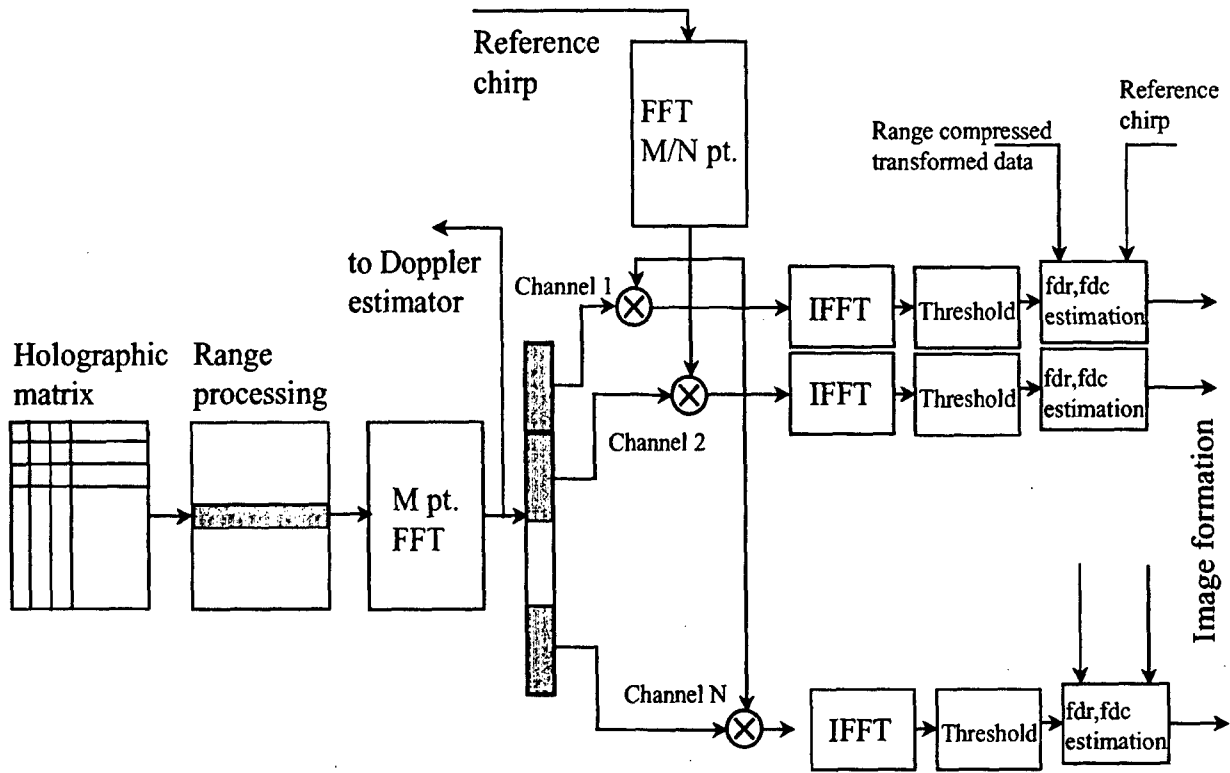


Figure 3: Processing scheme of MTDI (after [DDB94]).

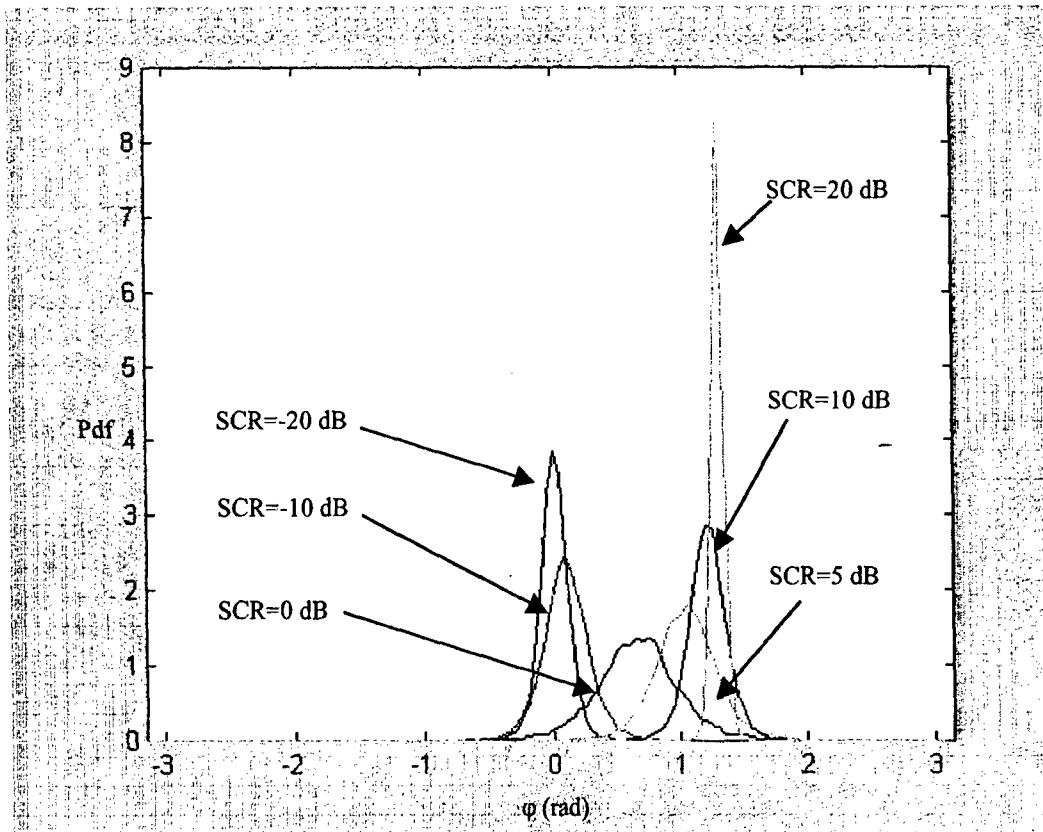


Figure 4: Histogram of phase interferogram.

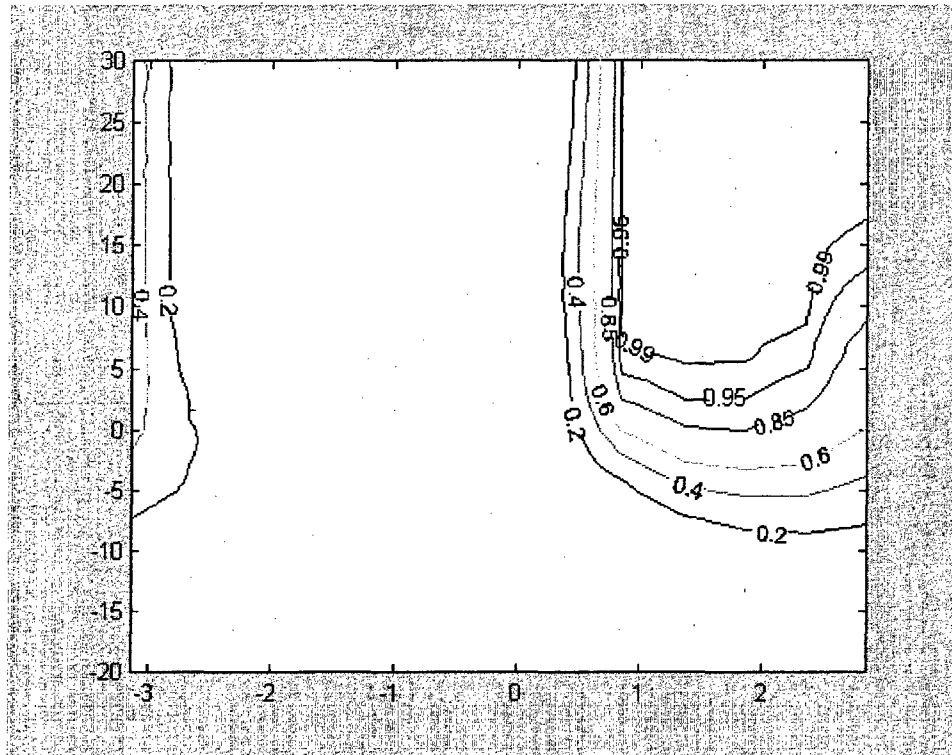
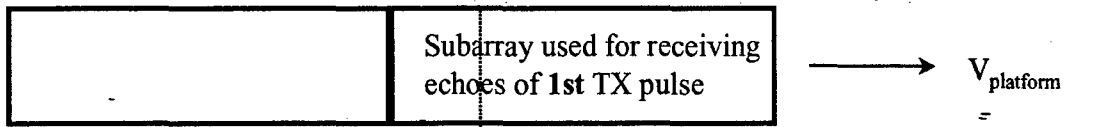


Figure 5: Contour curves with constant Pd versus target Doppler phase and signal to clutter power ratio.

TWO ELEMENT DPCA

Array position when the 1st pulse is transmitted



Array position when the 2nd pulse is transmitted

position of TX/RX phase centers for the two pulses

Figure 6: Working principle of DPCA.

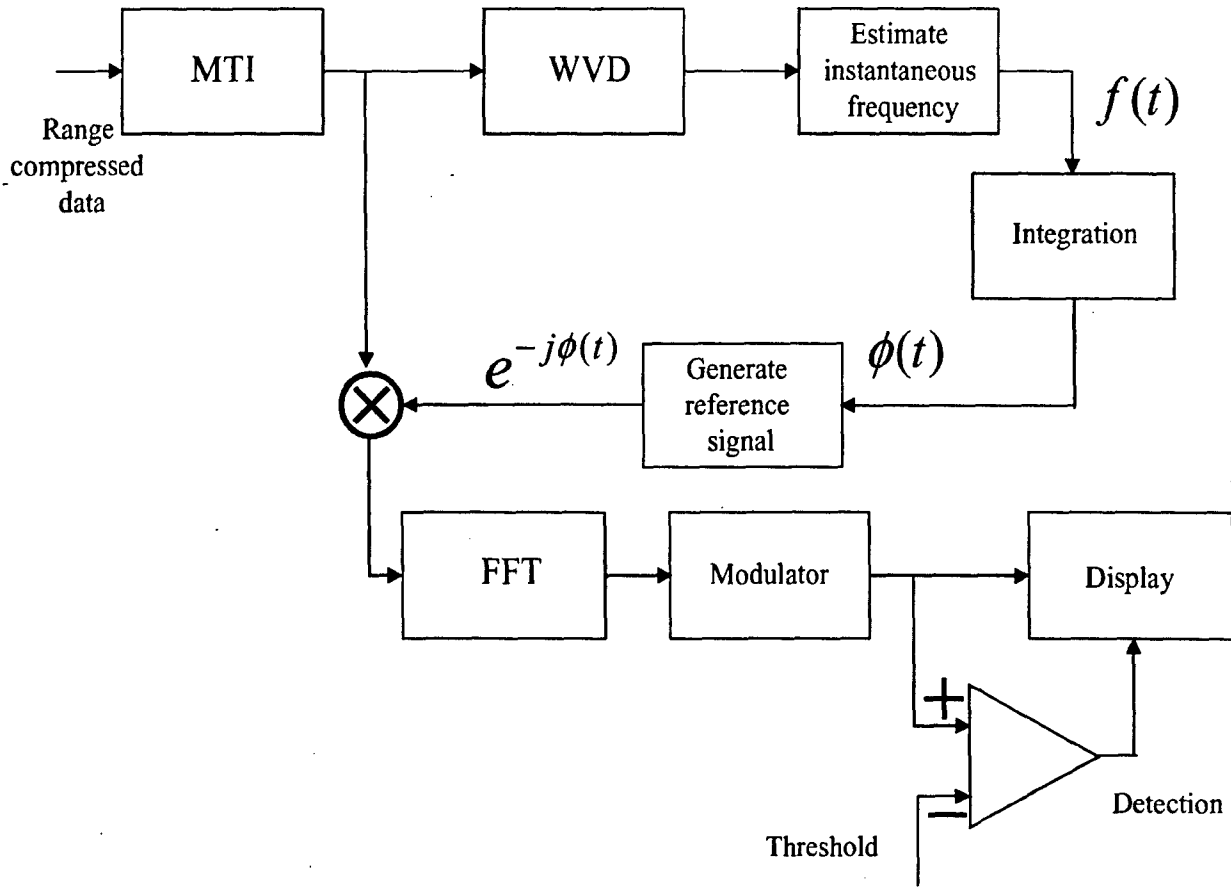


Figure 7: Processing scheme which uses the Wigner-Ville distribution.

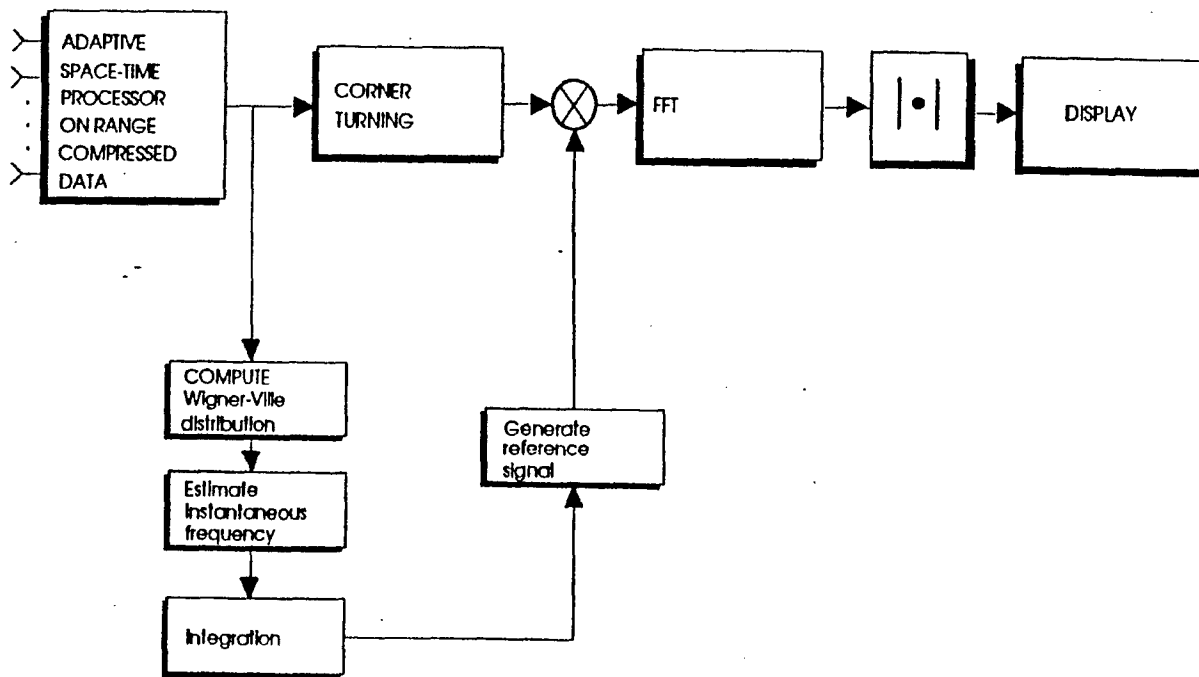


Figure 8. Processing scheme of joint space-time-frequency.

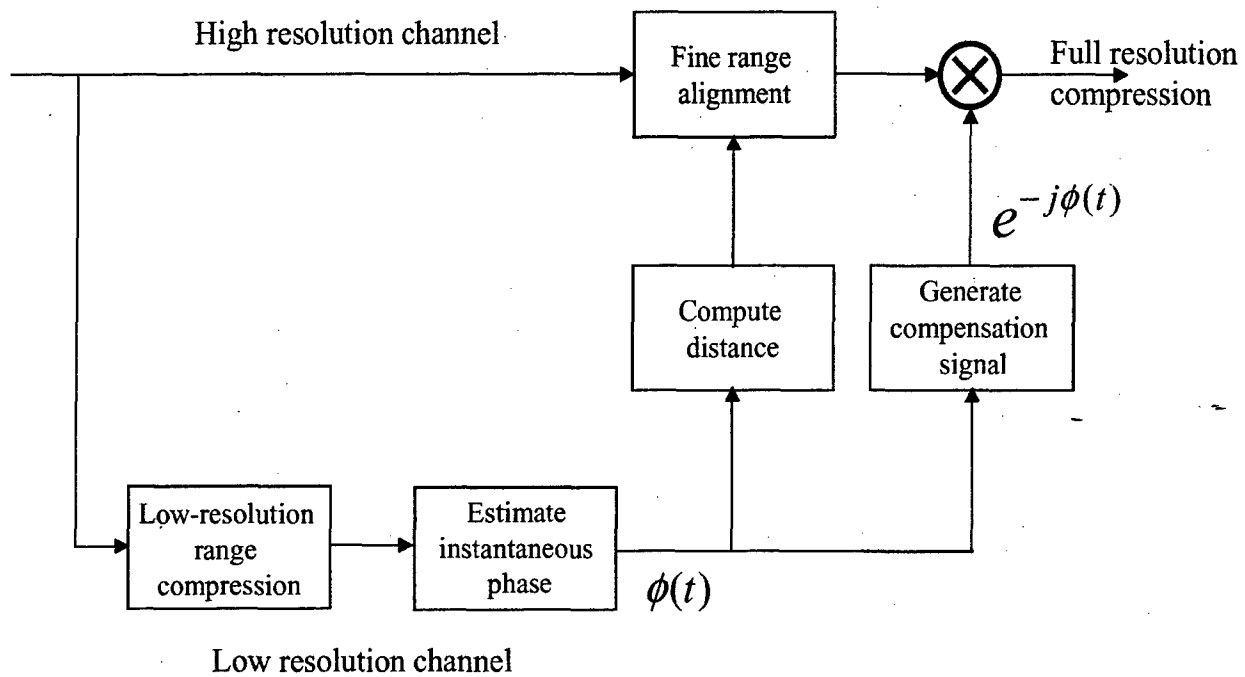


Figure 9: Two-step approach to account for range migration problem.